

## BASELINE STUDIES OF THE CLAY MINERALS SOCIETY SOURCE CLAYS: POWDER X-RAY DIFFRACTION ANALYSES

STEVE J. CHIPERA AND DAVID L. BISH

Geology and Geochemistry, MS D469, Los Alamos National Laboratory, Los Alamos, New Mexico 87545, USA

### INTRODUCTION

The Clay Minerals Society maintains a repository of Source Clays to provide scientists and researchers with a readily available supply of consistent materials so that research conducted by different groups can be correlated to identical material. These Source Clays include kaolinite, smectite, chlorite, vermiculite, illite, palygorskite and other minerals. As most of the Source Clays are naturally occurring materials, they typically contain minor to significant amounts of other mineral impurities. When conducting research using these samples, it is important that their mineral content be well characterized. It is also often desirable to remove these impurities to produce pure clay samples. For example, when studying the biological effects of a particular clay mineral, it is imperative that all contaminants (*e.g.* crystalline silica minerals) be removed from the clay in question so that experimental results can be attributed to the clay alone. If purification is required, the clays must be purified in a manner that does not significantly alter the physical or chemical properties of the samples. This chapter describes the X-ray diffraction (XRD) characteristics of a suite of Source Clays of The Clay Minerals Society and demonstrates methods of purification based on Stokes' law of settling in suspension that can be used to purify the clays.

### METHODS

We refer to samples obtained from P. Costanzo (see Costanzo, 2001) as 'processed' material and material obtained directly from the Source Clay Repository as 'as-shipped' material. Size fractionations and purifications were performed on the 'as-shipped' material to obtain the highest purity possible and to identify the impurities that occur in the material.

Powder XRD data were collected for the Source Clays on a Siemens D500 powder X-ray diffractometer using  $\text{CuK}\alpha$  radiation, incident- and diffracted-beam Soller slits, and a Kevex solid-state  $\text{Si}(\text{Li})$  detector. Data were collected from  $2$  to  $70^\circ 2\theta$  using a step size of  $0.02^\circ 2\theta$  and a count time of at least  $4$  s per step. All samples were analyzed as random (backpacked) mounts. In addition, experiments on smectite samples were made with oriented clay mineral aggregates prepared by suspending a sample in deionized water and pipetting the suspension onto an off-axis-

cut (zero background) quartz plate. Note that the resulting mounts are not infinitely thick, and the intensities of higher angle peaks are therefore weaker than otherwise for an infinitely thick sample. The XRD data for the oriented samples in this chapter should therefore be used as a guide to peak position only. Oriented mounts were analyzed under both ambient room conditions and after solvating overnight in an ethylene glycol atmosphere as outlined by Moore and Reynolds (1989). The smectite basal ( $00l$ )-diffraction pattern varies as a function of numerous factors, including the interlayer-cation type and relative humidity. Relative humidity during the ambient XRD experiments is reported in the respective figure captions.

Semi-quantitative mineral analyses used XRD data obtained from the random mounts and the 'external standard' method of Chung (1974). This method requires that reference intensity ratios (RIRs) be determined for each phase in the sample and that the sum of analyzed phases equals 100%. This latter requirement usually means that amorphous components are not quantified and the reported values may be overestimated. Although qualitative identification of the crystalline phases present can be accomplished quickly and accurately, quantitative multicomponent analysis is not straightforward and is complicated by numerous factors (*e.g.* Bish and Chipera, 1988). These factors include variations in degree of preferred orientation of the crystallites, relative humidity during the analysis, and Lorentz-polarization effects. A consistent RIR for the smectite  $00l$  reflection is difficult to obtain and can vary significantly, even for a given sample (Chipera and Bish, 1993). Consequently, mineral abundances reported in this study are semi-quantitative, although they provide a reasonable estimate of the purity of each sample.

Chipera *et al.* (1993) provided a generic procedure following Jackson (1979) for purifying/concentrating a clay sample without significantly altering the physical or chemical properties. This procedure involves suspending the sample in deionized water, disaggregating it using ultrasound, and settling (gravitationally and centrifugally) to extract progressively finer particle size-fractions. Clay minerals by their very nature are extremely fine grained, and it is this attribute that is utilized to separate them from more coarse-grained minerals with which they commonly coexist (quartz,

Table 1. The Clay Minerals Society Source Clays analyzed in this study.

Source Clay label	Clay mineral	Source Clay location
‘Processed’ <2 μm size-fraction samples		
KGa-1b	kaolinite	Washington County, GA
KGa-2	kaolinite	Warren County, GA
PFI-1	palygorskite	Gadsden County, FL
SAz-1	smectite	Cheto Mine, Apache County, AZ
STx-1	smectite	Gonzales County, TX
SWy-2	smectite	Crook County, WY
SHCa-1	hectorite	San Bernardino County, CA
Syn-1	synthetic mica-montmorillonite	Barasym SSM-100
‘As-shipped’ Clay Minerals Society Source Clays analyzed and purified in this study		
ISCz-1	illite-smectite (70/30 ordered)	Slovakia
ISMt-1	illite-smectite (60/40 ordered)	Mancos Shale (Cretaceous)
KGa-1	kaolinite	Washington County, GA
KGa-2	kaolinite	Warren County, GA
PFI-1	palygorskite	Gadsden County, FL
SAz-1	smectite	Cheto Mine, Apache County, AZ
SBCa-1	beidellite	California
SHCa-1	hectorite	San Bernardino County, CA
STx-1	smectite	Gonzales County, TX
SWa-1	ferruginous smectite	Grant County, WA
SWy-1	smectite	Crook County, WY

feldspar, calcite, *etc.*). Suspended material in the final supernatant liquid that was not removed during centrifugation (<0.1 μm in size) was recovered by evaporation at 50°C. It is prudent, however, to suspect that the characteristics of the fine clay particles are altered during evaporation (H<sup>+</sup>-exchange, altered surface charge, *etc.*). Other methods to remove the fine material from suspension include spray drying and freeze drying, although it is uncertain that these methods are less disturbing to the sample.

Chipera *et al.* (1993) noted numerous instances where deionized water alone does not adequately disperse a sample. This is evident when the coarser fraction does not settle out of suspension, but instead

slowly settles *en masse*, forming some rather interesting turbid forms and leaving a layer of clear water at the top. In these cases, a small amount (0.01 M) of Na hexametaphosphate [Na(PO<sub>3</sub>)<sub>6</sub>] may be added to the suspension as a dispersant, but there is a probability of cation exchange when using such dispersants. In addition, each size-fraction removed from suspension should be washed with deionized water at least three times to remove traces of the dispersant.

## RESULTS AND DISCUSSION

Figures 1–7 show the XRD patterns obtained for the ‘processed’ <2 μm size-fraction of the Source Clays. Figure 1 compares diffraction patterns obtained from

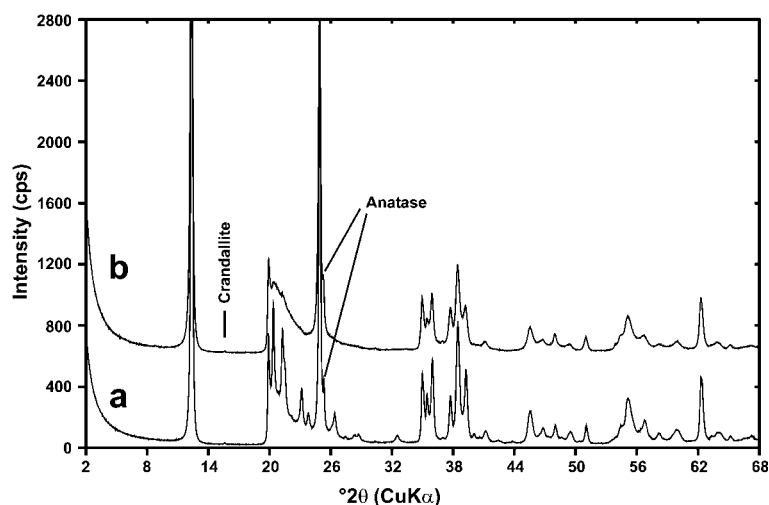


Figure 1. XRD patterns of the ‘processed’ <2 μm size-fraction of (a) KGa-1b and (b) KGa-2.

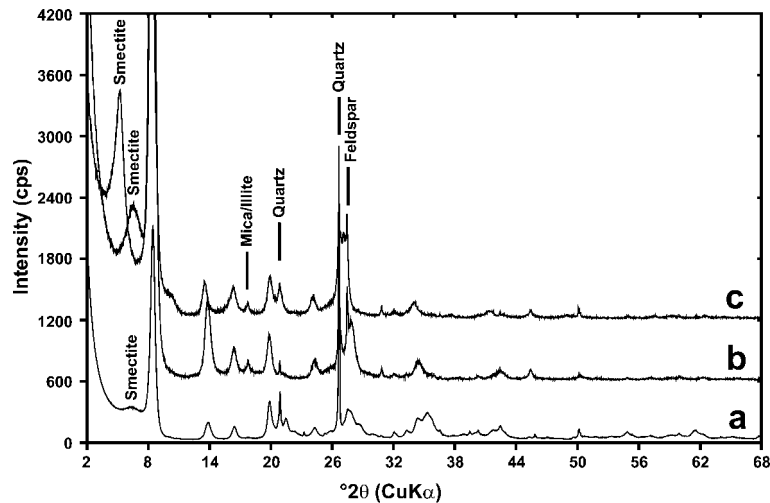


Figure 2. XRD patterns of the 'processed'  $<2 \mu\text{m}$  size-fraction of PFI-1 palygorskite: (a) random (collected at 24% RH;  $001_{\text{smectite}} = 13.8 \text{ \AA}$ ,  $110_{\text{palygorskite}} = 10.5 \text{ \AA}$ ); (b) oriented (collected at 5% RH;  $001_{\text{smectite}} = 13.5 \text{ \AA}$ ,  $110_{\text{palygorskite}} = 10.5 \text{ \AA}$ ); and (c) oriented and glycolated ( $001_{\text{smectite}} = 16.9 \text{ \AA}$ ,  $110_{\text{palygorskite}} = 10.7 \text{ \AA}$ ).

random mounts of the two kaolinites (KGa-1b and KGa-2). Figures 3–7 show the patterns of the smectite samples, with each figure providing results obtained from random, oriented and glycolated-oriented samples. Oriented and glycolated preparations of the palygorskite were also analyzed in addition to the random mount because of significant quantities of smectite in that sample (Figure 2).

With the exception of Syn-1, The Clay Minerals Society Source Clays are naturally occurring materials. As such, they often contain minor amounts of mineral impurities. For example, the kaolinite samples contain anatase ( $\text{TiO}_2$ ), palygorskite contains significant amounts of smectite and quartz, and the smectites contain quartz, feldspar, calcite and other impurities. Even

synthetic materials such as Syn-1 can contain impurities (Syn-1 contains boehmite). To assess whether any purification was accomplished during processing of the  $<2 \mu\text{m}$  size-fractions distributed to each of the authors in this volume, diffraction patterns were compared with those obtained on 'as-shipped' Source Clay material taken directly from the container. Semi-quantitative XRD analyses were conducted to determine the mineral abundances in both the 'processed'  $<2 \mu\text{m}$  size-fractions and the 'as-shipped' samples. These data are presented in Table 2. In most cases, processing to obtain the  $<2 \mu\text{m}$  size-fraction did little to alter the mineralogy of the samples. Note exceptions, however, for SWy-2 and SHCa-1 where significant purification of the samples was achieved.

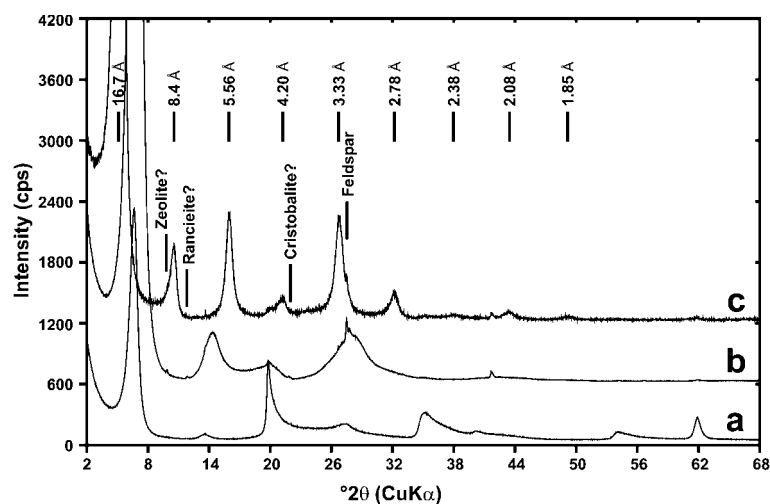


Figure 3. XRD patterns of the 'processed'  $<2 \mu\text{m}$  size-fraction of SAz-1 smectite: (a) random (collected at 6% RH;  $001 = 13.3 \text{ \AA}$ ); (b) oriented (collected at 3% RH;  $001 = 13.0 \text{ \AA}$ ); and (c) oriented and glycolated ( $001 = 16.7 \text{ \AA}$ ).

Table 2. Semi-quantitative XRD analyses of the CMS Source Clays showing the mineralogy of the 'processed' <2- $\mu$ m size-fraction samples and of the 'as-shipped' material and a listing of the impurities detected during purification of the 'as-shipped' material.

Source Clay label	Mineralogy of 'processed' <2 $\mu$ m size-fraction samples	Mineralogy of 'as-shipped' Source Clays	Impurities detected in the separates obtained during purification of the 'as-shipped' material
KGa-1	–	–	dickite, mica and/or illite, anatase, quartz, crandallite
KGa-1b	~96% kaolinite and trace dickite [3% anatase, 1% crandallite + quartz(?)]	~96% kaolinite and trace dickite [3% anatase, 1% crandallite + quartz(?)]	–
KGa-2	~96% kaolinite [3% anatase, 1% crandallite + mica and/or illite]	~96% kaolinite [3% anatase, 1% crandallite + mica and/or illite]	mica and/or illite, anatase, quartz, crandallite, feldspar(?)
PFl-1	~80% palygorskite [10% smectite, 7% quartz, 2% feldspar, 1% other]	~79% palygorskite [11% smectite, 6% quartz, 4% feldspar, 1% other]	smectite, quartz, mica and/or illite, feldspar, calcite
SAz-1	~99% smectite [1% other]	~98% smectite [1% quartz, 1% other]	feldspar, quartz, mica, magnetite, rancieite(?), cristobalite(?), zeolite(?), (amorphous? – glass or opal-A)
STx-1	~68% smectite [30% opal-CT, 2% quartz + feldspar + kaolinite + talc(?)]	~67% smectite [30% opal-CT, 3% quartz + feldspar + kaolinite + talc(?)]	opal-CT, quartz, kaolinite, feldspar, talc(?)
SWy-1	–	–	quartz, feldspar, mica and/or illite, calcite, hematite, kaolinite(?) and/or chlorite(?)
SWy-2	~95% smectite [4% quartz, 1% feldspar + gypsum + mica and/or illite + kaolinite(?) and/or chlorite(?)]	~75% smectite [8% quartz, 16% feldspar, 1% gypsum + mica and/or illite + kaolinite(?) and/or chlorite(?)]	–
SHCa-1	~97% smectite [2% calcite, 1% dolomite + kaolinite(?)]	~50% smectite [43% calcite, 3% dolomite, 3% quartz, 1% other]	calcite, dolomite, quartz, feldspar
Syn-1	~95% mica-montmorillonite [5% boehmite]	~95% mica-montmorillonite [5% boehmite]	–
ISCz-1	–	–	quartz, feldspar, kaolinite
ISMt-1	–	–	kaolinite, chlorite, mica and/or illite, gypsum, calcite, feldspar, quartz
SBCa-1	–	–	quartz, anatase, kaolinite, feldspar(?)
SWa-1	–	–	quartz, calcite(?)

– Not analyzed.

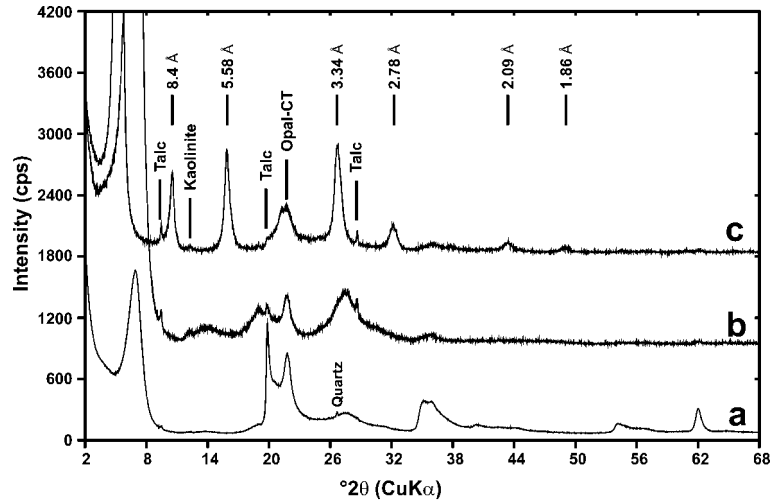


Figure 4. XRD patterns of the 'processed'  $<2 \mu\text{m}$  size-fraction of STx-1 smectite: (a) random (collected at 24% RH;  $001 = 12.8 \text{ \AA}$ ); (b) oriented (collected at 3% RH;  $001 = 12.7 \text{ \AA}$ ); (c) oriented and glycolated ( $001 = 16.8 \text{ \AA}$ ).

In addition to the 'processed'  $<2 \mu\text{m}$  size-fractions analyzed for this study, we include analyses of size separations conducted on 'as-shipped' Source Clays to demonstrate the purities obtained for these clays. Some of these separations were conducted prior to this study and are reported in Chipera *et al.* (1993). Although most of these original source materials continue to be distributed by The Clay Minerals Society, the sample lots of KGa-1 and SWy-1 are depleted and have been replaced by new lots (KGa-1b and SWy-2). Size separates were conducted on KGa-1 and SWy-1, but KGa-1b and SWy-2 were analyzed as the 'processed'  $<2 \mu\text{m}$  size-fraction samples in this study.

As a result of the separations conducted to concentrate/purify the Source Clays, mineral impurities that

previously went unnoticed in the bulk samples were often concentrated (generally in the coarsest or finest size-fractions) to levels where they could be detected more readily. The mineral impurities observed in the 'processed'  $<2 \mu\text{m}$  sized samples distributed for this study and in the clay separates conducted in the 'as-shipped' materials are listed in Table 2. Figures 8–14 show diffraction patterns for size separates from the 'as-shipped' Source Clays that were concentrated/purified using the methods outlined in Chipera *et al.* (1993). Generally, the separation method works well for removing quartz, feldspar and calcite from clay material containing predominantly smectite, kaolinite and zeolite, or for separating quartz and smectite from palygorskite. The method does not work well where

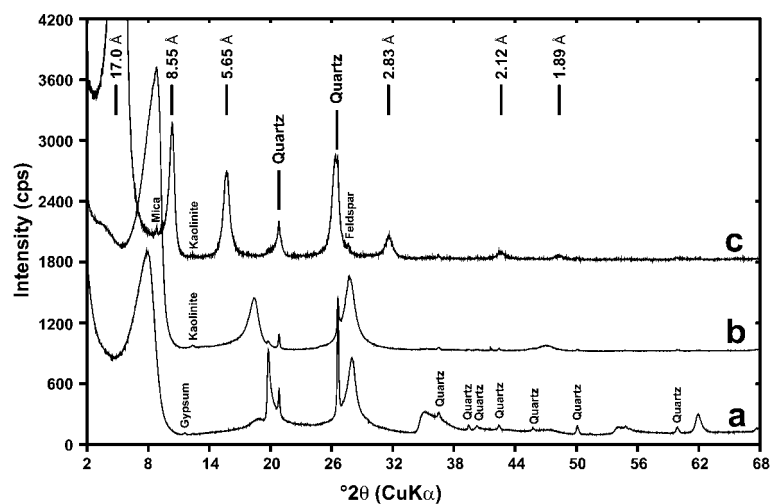


Figure 5. XRD patterns of the 'processed'  $<2 \mu\text{m}$  size-fraction of SWy-2 smectite: (a) random (collected at 9% RH;  $001 = 11.2 \text{ \AA}$ ); (b) oriented (collected at 3% RH;  $001 = 10.1 \text{ \AA}$ ); and (c) oriented and glycolated ( $001 = 17.0 \text{ \AA}$ ).

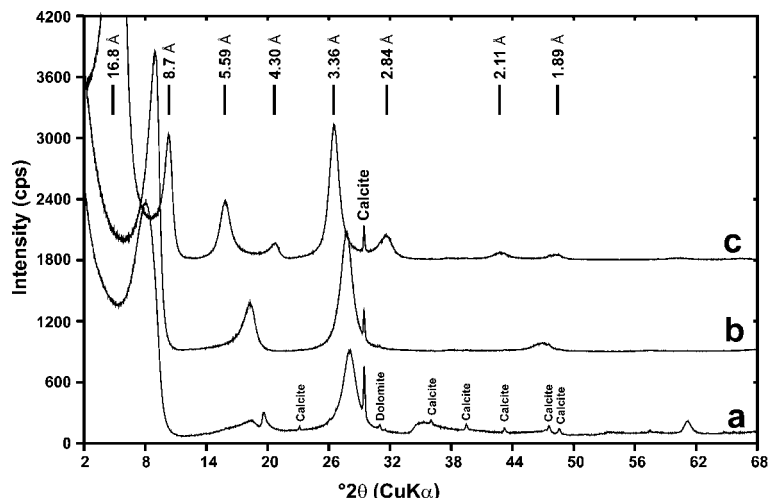


Figure 6. XRD patterns of the 'processed'  $<2 \mu\text{m}$  size-fraction of SHCa-1 hectorite: (a) random (collected at 6% RH;  $001 = 11.0 \text{ \AA}$ ); (b) oriented (collected at 5% RH;  $001 = 9.9 \text{ \AA}$ ); and (c) oriented and glycolated ( $001 = 16.8 \text{ \AA}$ ).

the physical attributes of an impurity closely match those of the mineral of interest or where the mineral of interest and the impurity are intergrown, *e.g.* STx-1 montmorillonite intergrown with opal-CT. The purification method worked well in removing illite and quartz from the kaolinite samples (Figures 8–9). Both the KGa-1 and KGa-2 kaolinite samples contain an impurity believed to be of the crandallite group, but the phase cannot be positively identified owing to the limited number of discrete reflections in the patterns. Interestingly, anatase did not behave identically in the size separations of the two kaolinite samples. The separation method concentrated anatase in the finer fractions of KGa-1 (Figure 8) but had little effect on the anatase concentration in the size-fractions of KGa-2 (Figure 9). Note that the degree of structural order

(defect density) in KGa-1 kaolinite varies as a function of particle size. KGa-1 is composed of at least two kaolinites with different defect densities (Bish and Chipera, 1998). It is significant that both KGa-1 and KGa-2 kaolinites have finer size-fractions which show no increased broadening of  $00l$  reflections, demonstrating that the coherent domain size is smaller than the particle size for the finest size-separate analyzed.

Figure 10 shows that the separation procedure can be used very effectively to remove quartz, mica and smectite impurities from PFI-1 palygorskite. The coarser quartz and feldspar particles settle more rapidly than the palygorskite, while the smectite particles remain in suspension. Figures 11, 12 and 13 show the diffraction patterns for the size-fractions obtained on

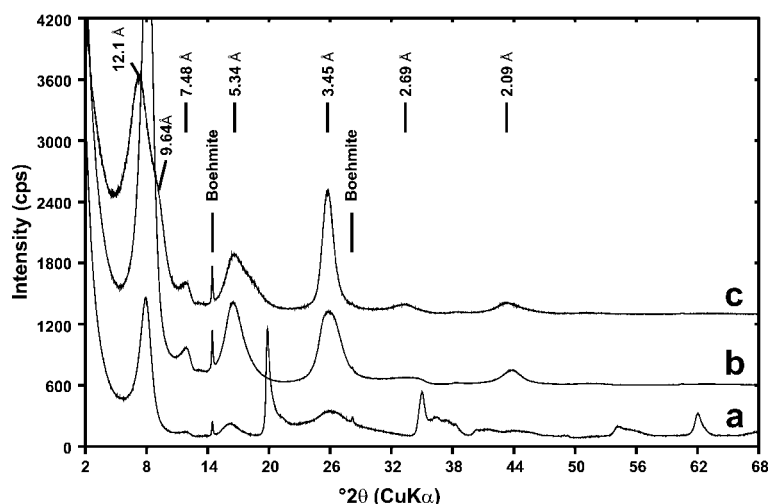


Figure 7. XRD patterns of the 'processed'  $<2 \mu\text{m}$  size-fraction of Syn-1 mica-montmorillonite: (a) random (collected at 11% RH;  $001 = 11.2 \text{ \AA}$ ); (b) oriented (collected at 5% RH;  $001 = 10.9 \text{ \AA}$ ); and (c) oriented and glycolated ( $001 = 12.1 \text{ \AA}$ ).

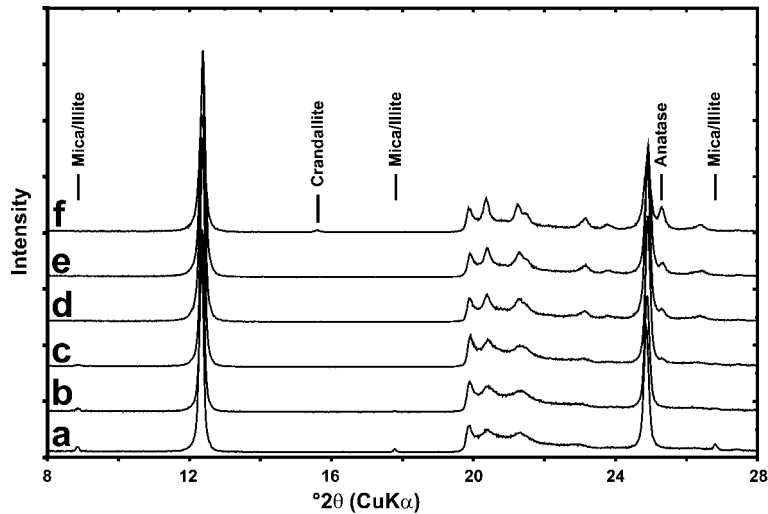


Figure 8. XRD patterns of size-fractions of KGa-1 kaolinite separated using 0.01 M Na hexametaphosphate solution. Fraction A: gravity settled for 1 min ( $>40\ \mu\text{m}$ ); Fraction B: gravity settled for an additional 5 min ( $18\text{--}40\ \mu\text{m}$ ); Fraction C: gravity settled for an additional 60 min ( $5\text{--}18\ \mu\text{m}$ ); Fraction D: gravity settled for an additional 64 h ( $0.7\text{--}5\ \mu\text{m}$ ); Fraction E: centrifuged using a Sorvall GSA head at 5000 RPM for 5 min ( $0.25\text{--}0.7\ \mu\text{m}$ ); and Fraction F: centrifuged using a Sorvall GSA head at 8000 RPM for 40 min ( $0.1\text{--}0.25\ \mu\text{m}$ ).

SAz-1, STx-1 and SWy-1, respectively. In all these clays, the finer size-fractions consist of mostly pure smectite. The patterns for the SWy-1 fractions (Figure 13) show an additional reflection at  $\sim 23.8\ \text{\AA}$ . Likewise, this reflection is observed in the pattern for the oriented sample of SWy-2 (Figure 5b). These patterns were all collected during the winter months at low ambient relative humidity (2–5% RH). Moore and Hower (1986) observed this reflection during a study of hydration and dehydration of SWy-1 and determined that it is

the result of an ordered interstratification of dehydrated ( $9.6\ \text{\AA}$ ) smectite and smectite with one water layer ( $12.4\ \text{\AA}$ ). Such an ordered interstratification will yield an effective  $00l$  repeat of  $22.0\ \text{\AA}$ , which results in a slightly larger  $00l$  spacing after correction by the Lorentz factor.

Figure 14 shows that a very pure sample can be obtained from SHCa-1 hectorite, although centrifugation is required to remove the significant amounts of calcite, quartz and dolomite. Figures 15–18 show sim-

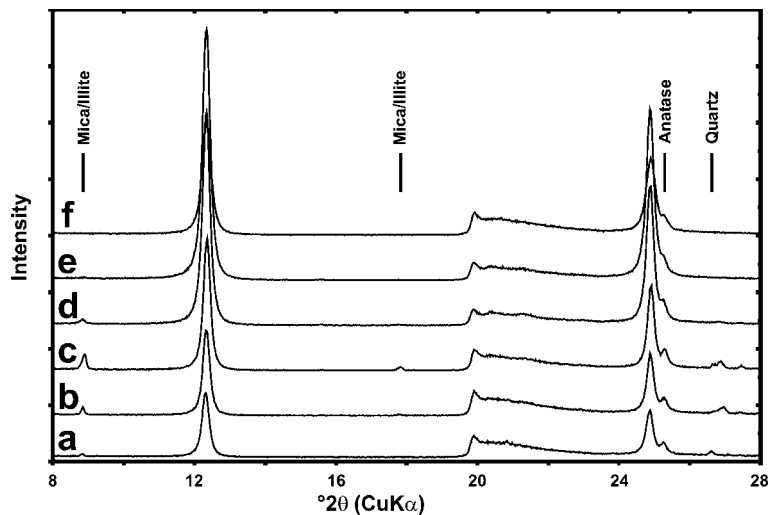


Figure 9. XRD patterns of size-fractions of KGa-2 kaolinite separated using 0.01 M Na hexametaphosphate solution. Fraction A: gravity settled for 1 min ( $>40\ \mu\text{m}$ ); Fraction B: gravity settled for an additional 5 min ( $18\text{--}40\ \mu\text{m}$ ); Fraction C: gravity settled for an additional 60 min ( $5\text{--}18\ \mu\text{m}$ ); Fraction D: gravity settled for an additional 64 h ( $0.7\text{--}5\ \mu\text{m}$ ); Fraction E: centrifuged using a Sorvall GSA head at 5000 RPM for 5 min ( $0.25\text{--}0.7\ \mu\text{m}$ ); and Fraction F: centrifuged using a Sorvall GSA head at 8000 RPM for 40 min ( $0.1\text{--}0.25\ \mu\text{m}$ ).

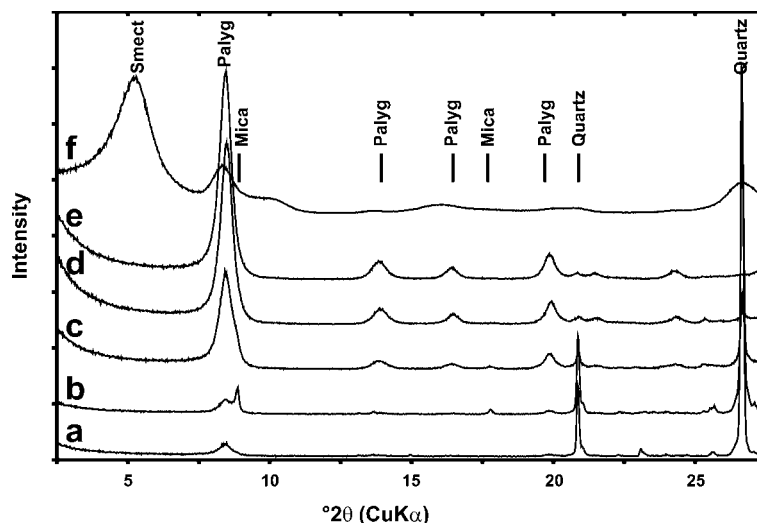


Figure 10. XRD patterns of size-fractions of PF1-1 palygorskite separated using 0.01 M Na hexametaphosphate solution. Fraction A: gravity settled for 5 min ( $>18 \mu\text{m}$ ); Fraction B: gravity settled for an additional 60 min ( $5\text{--}18 \mu\text{m}$ ); Fraction C: centrifuged using a Sorvall GSA head at 3000 RPM for 5 min ( $0.35\text{--}5 \mu\text{m}$ ); Fraction D: centrifuged using a Sorvall GSA head at 8000 RPM for 5 min ( $0.15\text{--}0.35 \mu\text{m}$ ); Fraction E: centrifuged using a Sorvall GSA head at 8000 RPM for 40 min ( $0.1\text{--}0.15 \mu\text{m}$ ); and Fraction F: evaporated supernatant liquid ( $<0.1 \mu\text{m}$ ).

ilar results for the Special Clays, ISCz-1, ISMt-1, SBCa-1 and SWa-1. Again, these clays can be purified effectively, with the coarser-grained impurities remaining in the larger-grain size-fractions.

#### ACKNOWLEDGMENTS

We are grateful to S. Guggenheim, R. Reynolds, Jr. and D. Vaniman for their helpful comments.

#### REFERENCES

- Bish, D.L. and Chipera, S.J. (1988) Problems and solutions in quantitative analysis of complex mixtures of X-ray powder diffraction. Pp. 295–308 in *Advances in X-Ray Analysis*, Volume 31 (C.S. Barrett, J.V. Gilfrich, R. Jenkins, J.C. Russ, J.W. Richardson, Jr. and P.K. Predecki, editors). Plenum Press, New York.
- Bish, D.L. and Chipera, S.J. (1998) Variation of kaolinite defect structure with particle size. *Proceedings of the 35th Annual Clay Minerals Society Meeting, Cleveland, Ohio*, p. 90.
- Chipera, S.J. and Bish, D.L. (1993) Effects of humidity on clay and zeolite quantitative XRD analyses. *Proceedings of the 30th Annual Clay Minerals Society Meeting, San Diego, California*, p. 53.
- Chipera, S.J., Guthrie, G.D. Jr. and Bish, D.L. (1993) Preparation and purification of mineral dusts. Pp. 235–249 in: *Health Effects of Mineral Dusts* (G.D. Guthrie and B.T. Mossman, editors). Reviews in Mineralogy, **28**. Mineralogical Society of America, Washington, D.C.
- Chung, F.H. (1974) Quantitative interpretation of X-ray diffraction patterns of mixtures. II. Adiabatic principle of X-ray diffraction analysis of mixtures. *Journal of Applied Crystallography*, **7**, 526–531.
- Costanzo, P. (2001) Baseline studies of the Clay Minerals Society Source Clays: introduction. *Clays and Clay Minerals*, **49**, 372–373.
- Jackson, M.L. (1979) *Soil Chemical Analysis—Advanced Course, 2nd Edition*. Published by the author, Madison, Wisconsin.
- Moore, D.M. and Hower, J. (1986) Ordered interstratification of dehydrated and hydrated Na-smectite. *Clays and Clay Minerals*, **34**, 379–384.
- Moore, D.M. and Reynolds, R.C., Jr. (1989) *X-Ray Diffraction and the Identification and Analysis of Clay Minerals*. Oxford University Press, New York, 332 pp.

E-mail of corresponding author: chipera@lanl.gov

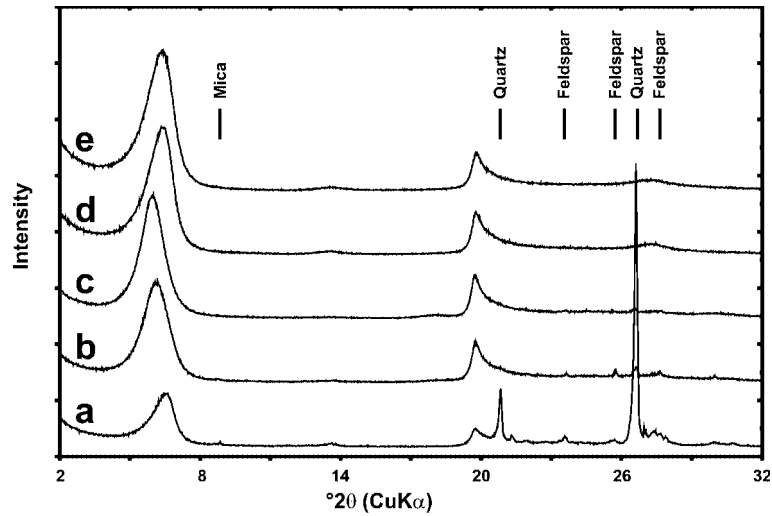


Figure 11. XRD patterns of size-fractions of SAz-1 montmorillonite separated using deionized water only. Fraction A: gravity settled for 5 min ( $>18 \mu\text{m}$ ); Fraction B: gravity settled for an additional 60 min ( $5\text{--}18 \mu\text{m}$ ); Fraction C: gravity settled for an additional 16 h ( $1.5\text{--}5 \mu\text{m}$ ); Fraction D: centrifuged using a Sorvall GSA head at 5000 RPM for 5 min ( $0.25\text{--}1.5 \mu\text{m}$ ); and Fraction E: centrifuged using a Sorvall GSA head at 8000 RPM for 60 min ( $0.1\text{--}0.25 \mu\text{m}$ ).

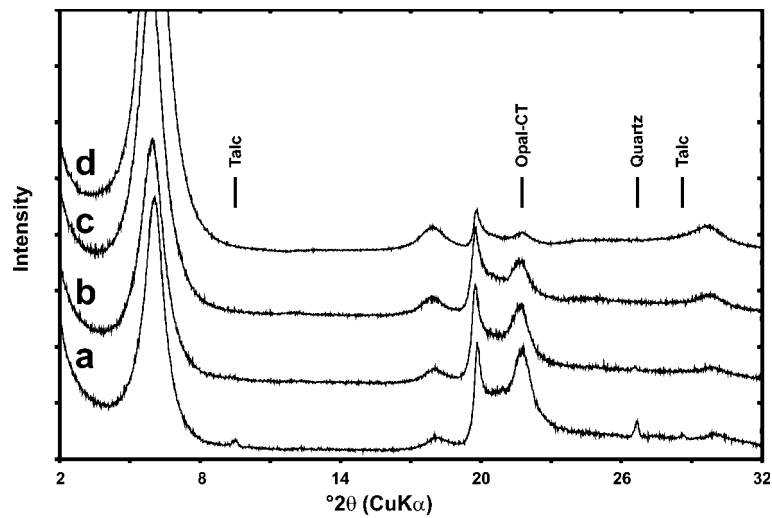


Figure 12. XRD patterns of size-fractions of STx-1 montmorillonite separated using deionized water only. Fraction A: gravity settled after 5 min for an additional 16 h ( $1.5\text{--}18 \mu\text{m}$ ); Fraction B: centrifuged using a Sorvall GSA head at 5000 RPM for 5 min ( $0.25\text{--}1.5 \mu\text{m}$ ); Fraction C: centrifuged using a Sorvall GSA head at 8000 RPM for 40 min ( $0.1\text{--}0.25 \mu\text{m}$ ); and Fraction D: evaporated supernatant liquid ( $<0.1 \mu\text{m}$ ).

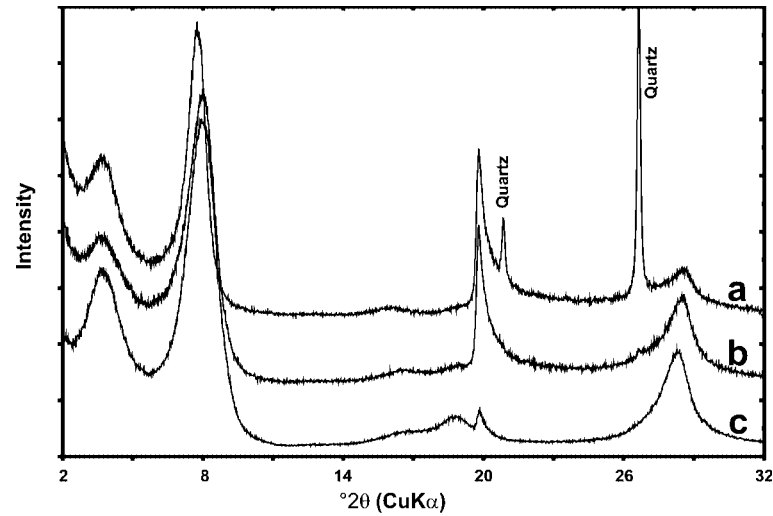


Figure 13. XRD patterns of size-fractions of SWy-1 montmorillonite separated using deionized water only. Fraction A: centrifuged using a Sorvall GSA head at 5000 RPM for 5 min after centrifuging at 3000 RPM for 5 min (0.25–0.4  $\mu\text{m}$ ); Fraction B: centrifuged using a Sorvall GSA head at 8000 RPM for 60 min (0.1–0.25  $\mu\text{m}$ ); and Fraction C: evaporated supernatant liquid (<0.1  $\mu\text{m}$ ).

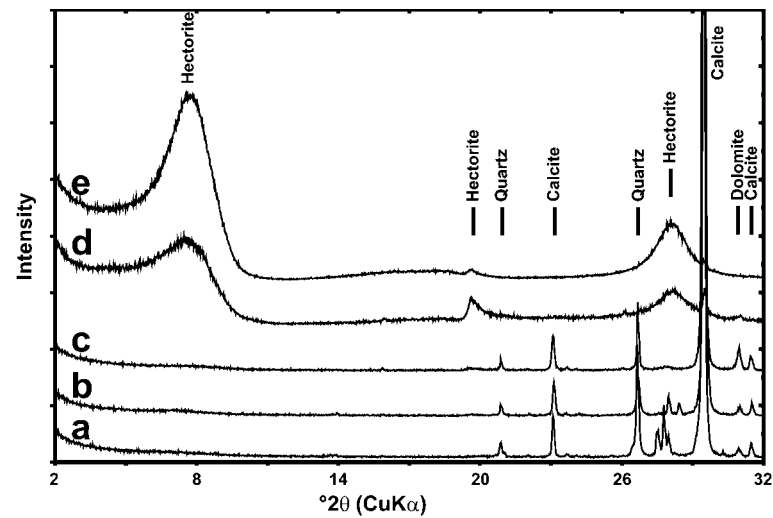


Figure 14. XRD patterns of size-fractions of SHCa-1 hectorite separated using deionized water only. Fraction A: gravity settled for 5 min (>18  $\mu\text{m}$ ); Fraction B: gravity settled for an additional 60 min (5–18  $\mu\text{m}$ ); Fraction C: centrifuged using a Sorvall GSA head at 5000 RPM for 5 min (0.25–5  $\mu\text{m}$ ); Fraction D: centrifuged using a Sorvall GSA head at 8000 RPM for 60 min (0.1–0.25  $\mu\text{m}$ ); and Fraction E: evaporated supernatant liquid (<0.1  $\mu\text{m}$ ).

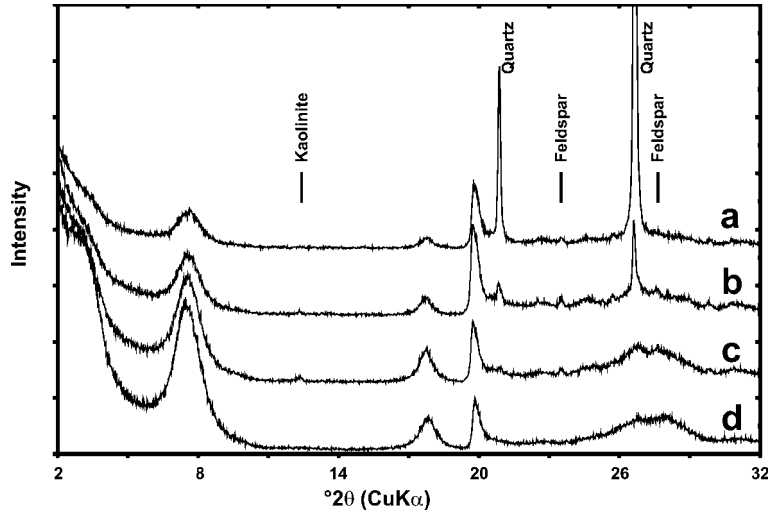


Figure 15. XRD patterns of size-fractions of ISCz-1 illite-smectite separated using deionized water only. Fraction A: gravity settled after 5 min for an additional 60 min (5–18  $\mu\text{m}$ ); Fraction B: gravity settled for an additional 16 h (1.5–5  $\mu\text{m}$ ); Fraction C: centrifuged using a Sorvall GSA head at 5000 RPM for 5 min (0.25–1.5  $\mu\text{m}$ ); and Fraction D: centrifuged using a Sorvall GSA head at 8000 RPM for 40 min (0.1–0.25  $\mu\text{m}$ ).

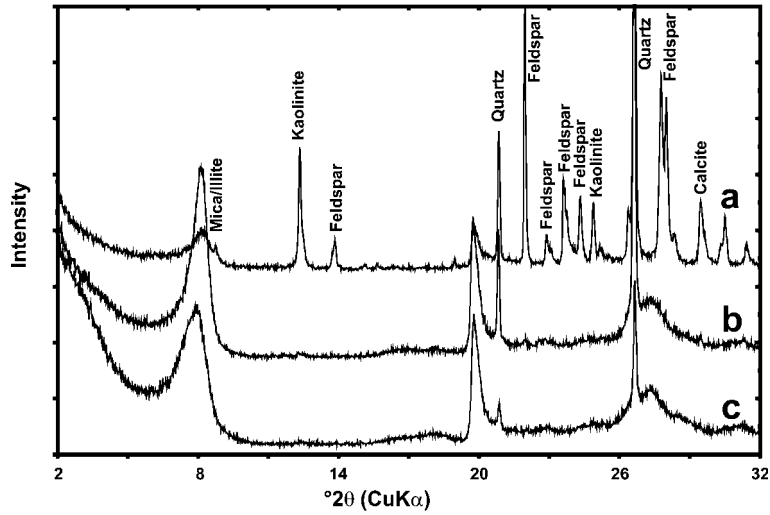


Figure 16. XRD patterns of size-fractions of ISMt-1 illite-smectite separated using deionized water only. Fraction A: gravity settled after 5 min for an additional 60 min (5–18  $\mu\text{m}$ ); Fraction B: gravity settled for an additional 64 h (0.7–5  $\mu\text{m}$ ); and Fraction C: centrifuged using a Sorvall GSA head at 5000 RPM for 5 min (0.25–0.7  $\mu\text{m}$ ).

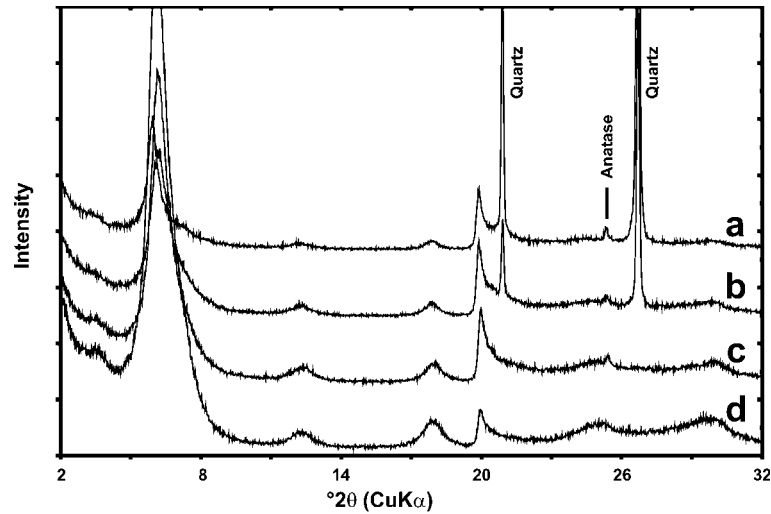


Figure 17. XRD patterns of size-fractions of SBCa-1 beidellite separated using deionized water only. Fraction A: gravity settled after 5 min for an additional 60 min (5–18  $\mu\text{m}$ ); Fraction B: gravity settled for an additional 16 h (1.5–5  $\mu\text{m}$ ); Fraction C: centrifuged using a Sorvall GSA head at 5000 RPM for 5 min (0.25–1.5  $\mu\text{m}$ ); and Fraction D: centrifuged using a Sorvall GSA head at 8000 RPM for 40 min (0.1–0.25  $\mu\text{m}$ ).

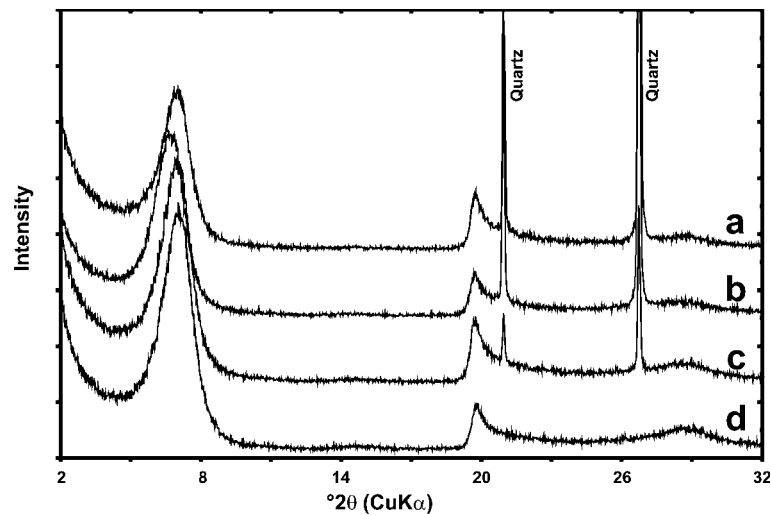


Figure 18. XRD patterns of size-fractions of SWa-1 ferruginous smectite separated using deionized water only. Fraction A: gravity settled after 5 min for an additional 60 min (5–18  $\mu\text{m}$ ); Fraction B: gravity settled for an additional 64 h (0.7–5  $\mu\text{m}$ ); Fraction C: centrifuged using a Sorvall GSA head at 5000 RPM for 5 min (0.25–0.7  $\mu\text{m}$ ); and Fraction D: centrifuged using a Sorvall GSA head at 8000 RPM for 60 min (0.1–0.25  $\mu\text{m}$ ).